Redox Biology 26 (2019) 101258

Contents lists available at ScienceDirect

Redox Biology

journal homepage: www.elsevier.com/locate/redox

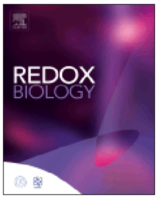

Research Paper

Catalyst-free Click PEGylation reveals substantial mitochondrial ATP synthase sub-unit alpha oxidation before and after fertilisation

James N. Cobley[a,*], Anna Noble[b], Eduardo Jimenez-Fernandez[a], Manuel-Thomas Valdivia Moya[a], Matthew Guille[b], Holger Husi[a]

[a] Free Radical Research Group, University of the Highlands and Islands, Centre for Health Sciences, Inverness, IV2 3JH, UK
[b] European Xenopus Resource Centre, University of Portsmouth, School of Biological Sciences, King Henry Building, Portsmouth, PO1 2DY, UK

ARTICLE INFO

Keywords:
Mitochondria
ATP synthase
Fertilisation
Development
Redox signalling

ABSTRACT

Using non-reducing Western blotting to assess protein thiol redox state is challenging because most reduced and oxidised forms migrate at the same molecular weight and are, therefore, indistinguishable. While copper catalysed Click chemistry can be used to ligate a polyethylene glycol (PEG) moiety termed Click PEGylation to mass shift the reduced or oxidised form as desired, the potential for copper catalysed auto-oxidation is problematic. Here we define a catalyst-free *trans*-cyclooctene-methyltetrazine (TCO-Tz) inverse electron demand Diels Alder chemistry approach that affords rapid (k ~2000 $M^{-1} s^{-1}$), selective and bio-orthogonal Click PEGylation. We used TCO-Tz Click PEGylation to investigate how fertilisation impacts reversible mitochondrial ATP synthase F_1-F_o sub-unit alpha (ATP-α-F_1) oxidation—an established molecular correlate of impaired enzyme activity—in *Xenopus laevis.* TCO-Tz Click PEGylation studies reveal substantial (~65%) reversible ATP-α-F_1 oxidation at evolutionary conserved cysteine residues (i.e., C^{244} and C^{294}) before and after fertilisation. A single thiol is, however, preferentially oxidised likely due to greater solvent exposure during the catalytic cycle. Selective reduction experiments show that: S-glutathionylation accounts for ~50–60% of the reversible oxidation observed, making it the dominant oxidative modification type. Intermolecular disulphide bonds may also contribute due to their relative stability. Substantial reversible ATP-α-F_1 oxidation before and after fertilisation is biologically meaningful because it implies low mitochondrial F_1-F_o ATP synthase activity. Catalyst-free TCO-Tz Click PEGylation is a valuable new tool to interrogate protein thiol redox state in health and disease.

1. Introduction

Much mitochondrial redox biology from apoptosis and oxidative phosphorylation to uncoupling can be ascribed to matrix superoxide anion ($O_2^{\cdot-}$) and hydrogen peroxide (H_2O_2) [1–8]. Matrix $O_2^{\cdot-}$/H_2O_2 may signal via intermediate thiyl radicals and sulfenic acids (SOH) [9–12], species that establish a chemical route to covalent oxidative modifications capable of altering protein function (i.e., disulphide bonds, S-glutathionylation and S-nitrosation [13–20]). The emerging consensus from redox proteomic studies is that: reversible protein thiol oxidation regulates respiratory chain complex activity (reviewed in Ref. [21]). To give a key example, S-nitrosation of a single cysteine in ND3 (Cys^{39}) protects against ischemia-reperfusion injury induced $O_2^{\cdot-}$ production by locking complex I in a structurally inactive state [22–24]. Despite their many advantages, redox proteomic approaches are often unsuitable for addressing many hypothesis-driven questions [25,26]. Using non-reducing Western blotting to address hypothesis-driven questions is challenging because the reduced and oxidised forms of most protein thiols possess similar electrophoretic mobility. Functionalising maleimide with a polyethylene glycol (PEG) moiety can impart a mass shift to the reduced or oxidised form [27]. The bulky PEG moiety may, however, sterically impede thiol labelling [26].

Recently, van Leeuwen and colleagues [26] described a novel Click chemistry approach (termed Click PEGylation) that bypasses steric concerns by making the thiol labelling step PEG independent. To detect oxidised protein thiols they exploited copper (Cu^+) catalysed Click chemistry [28] wherein alkyne-maleimide is ligated to a low molecular weight (e.g., 5 kDa) azide-PEG moiety to form a stable triazole. The oxidised form migrates at a higher molecular weight compared with the reduced form owing to the azide-PEG moiety induced redox mobility shift, which is detectable by Western blotting [26]. However, the need for a cytotoxic catalyst that requires additional reductants (e.g., L-ascorbic acid) and stabilisers (e.g., tris [(1-benzyl-1H-1,2,3,-triazol-4-yl) methyl] amine) is problematic. For example, Cu^+ could adventitiously

---

[*] Corresponding author.
E-mail address: james.cobley@uhi.ac.uk (J.N. Cobley).

https://doi.org/10.1016/j.redox.2019.101258
Received 20 May 2019; Received in revised form 10 June 2019; Accepted 15 June 2019

auto-oxidise samples [29]. One can omit Cu^+ entirely using catalyst-free *trans*-cyclooctene-methyltetrazine (TCO-Tz) pair inverse electron demand Diels Alder chemistry [30,31]. The electron rich dienophile TCO reacts with the electron poor diene methyltetrazine to yield a conjugated pyridazine product via strained 4,5-dihydropyridazine and 1,4-dihydro-isomer intermediates [32]. TCO-Tz inverse electron demand Diels Alder chemistry is rapid (k ~2000 $M^{-1} s^{-1}$), selective and bio-orthogonal [33]. The rate constant corresponds to a ~10-000 fold enhancement over Cu^+ catalysed Click chemistry [32]. TCO-Tz Click PEGylation could help unravel how key biological phenomena (e.g., fertilisation) impact protein thiol redox state.

Fertilisation induces mitochondrial H_2O_2 release [34–36], but whether fertilisation impacts reversible protein thiol oxidation is an open question. This is important because thiol oxidation is a post-translational modification that can act as a negative regulator of mitochondrial ATP synthesis (see below). ATP demand appears to be comparatively low in the unfertilised egg before fertilisation initiates embryonic metabolism by increasing ATP expenditure [37]. ATP is required to support the biosynthetic demands of embryogenesis [38]. Existing knowledge suggests a mechanism of tuning ATP synthesis rate within the F_1-F_o mitochondrial ATP synthase itself by reversibly oxidising the cognate ATP F_1 alpha sub-unit (ATP-α-F_1, reviewed in Refs. [39–41]). ATP-α-F_1 is an integral component of a matrix facing multi sub-unit assembly responsible for chemiosmotic ATP synthesis [42–44]. In particular, arginine 373 helps stabilise transition states [45]. Reversible ATP-α-F_1 oxidation was first demonstrated in 2006 by West and colleagues [46] and confirmed by redox proteomic studies showing that $C^{244/294}$ are subject to S-glutathionylation and S-nitrosation [47–49]. Reversible ATP-α-F_1 oxidation is an established molecular correlate of impaired catalysis [47]. Interestingly, ADP provides an instructive cue to restore catalytic activity by reversing thiol oxidation [48]. Inhibitory ATP-α-F_1 oxidation may constrain ATP synthesis to preserve finite resources in the unfertilised egg before ADP provides a signal to increase mitochondrial ATP synthesis after fertilisation. We aimed to determine whether fertilisation alters ATP-α-F_1 redox state in *Xenopus laevis* (*X. laevis*), an important developmental model [50–52], using TCO-Tz Click chemistry. Fertilisation induces H_2O_2 release in *X. laevis* mitochondria [34], making them an ideal model to test our experimental hypothesis that: reversible ATP-α-F_1 oxidation is greater in the unfertilised egg than in the 1-cell embryo.

2. Methods

2.1. Materials and reagents

A complete list of the materials and reagents used is provided (see Supplementary Table 1).

2.1.1. Xenopus laevis

In-house bred *X. laevis* were maintained at the European *Xenopus* Resource Centre (EXRC) at 18 °C and fed daily on trout pellets (see https://xenopusresource.org/). Following ethical approval (#OLETH-SHE1500), unfertilised eggs *X. laevis* were harvested. *X. laevis* embryos were dejellied and then harvested either immediately (designated as 15 min) or 90 min post *in vitro* fertilisation (IVF) [53]. IVF was performed according to standard *X. laevis* protocols [54]. Samples were stored at −80 °C until biochemical analysis. The 5 and 90 min time points were selected to capture redox changes as soon as practically possible after fertilisation and the first embryonic cell cycle, respectively [34]. To minimise the possibility that our results were attributable to any one female or outliers [55], samples were obtained from three adult females and unfertilised eggs/embryos were grouped into batches of five for biochemical analysis.

2.1.2. Click PEG_{OX} protocol

Samples were homogenised in ice-cold lysis buffer (150 mM NaCl, 10 mM EDTA, 100 mM Tris, 1% Triton X-100, pH 7.2) supplemented with a protease inhibitor tablet (Sigma, UK, #11697498001) and 100 mM N-ethylmaleimide (NEM; Sigma, UK, #E3876). Homogenates were left to stand for 30 min on ice to enable NEM to alkylate reduced thiols, before being centrifuged at 14,000 *g* for 5 min at 4 °C. After performing a Bradford assay to determine protein content [56], samples were adjusted to 1000 μg/ml to normalise protein concentration. Samples were then passed through a 6000 kDa spin column (BioRad, UK, Micro Bio-Spin™ P-6 Gel Columns, #7326222) to remove excess NEM. The flow-through was treated with 5 mM Tris (2-carboxyethyl)phosphine hydrochloride (TCEP; Thermofisher Scientific, UK, #T2556) for 30 min on ice to reduce reversibly oxidised thiols. A spin column step was incorporated to prevent TCEP from interfering with subsequent thiol labelling [57]. *Trans*-cyclooctene (TCO)-3 polyethylene glycol (PEG)-maleimide (TCO-PEG3-NEM, Click Chemistry Tools, USA, #1002) was added (5 mM) to label newly reduced thiols for 30 min on ice. To initiate the Click reaction, 5 mM 6-methyltetrazine 5 kDa PEG (Tz-PEG5; Click Chemistry Tools, USA #1090) was added for 60 min at room temperature with gentle agitation. Samples were then passed through a 6000 kDa spin column to prevent excess PEG smearing gel bands by forming micelles with SDS [58]. To obtain a maximally oxidised control, samples were lysed with 50 mM diamide (Sigma, UK, #D3648) to oxidise thiols, centrifuged at 14,000 *g* for 5 min at 4 °C and the supernatant was passed through a 6000 kDa spin column to remove excess diamide. The TCO-Tz Click reaction was terminated by adding Laemmli buffer (4% SDS, 20% glycerol, 0.004% bromphenol blue and 0.125 M Tris, pH 6.8) supplemented with 100 mM 1,4-Dithiothreitol (DTT, VWR, UK, #443853 B), before samples were denatured at 80 °C for 5 min [59].

2.1.3. Click PEG_{RED} protocol

Samples were homogenised in the presence of 100 mM TCO-PEG3-NEM. Homogenates were left to stand for 30 min on ice to enable TCO-PEG3-NEM to label reduced thiols, before being centrifuged at 14,000 *g* for 5 min at 4 °C. After determining protein content [56], samples were adjusted to 1000 μg/ml to normalise starting protein concentration. To initiate the Click reaction, 5 mM Tz-PEG5 was added for 60 min at room temperature with gentle agitation. Samples were then passed through a 6000 kDa spin column to remove excess Tz-PEG5. To obtain a maximally reduced control, samples were lysed with 50 mM TCEP to reduce reversibly oxidised thiols, centrifuged at 14,000 *g* for 5 min at 4 °C and the supernatant was passed through a 6000 kDa spin column to remove excess TCEP. The TCO-Tz Click reaction was terminated by adding Lammeli buffer supplemented with 100 mM DTT, before samples were denatured at 80 °C for 5 min [59].

2.1.4. Selective S-glutathionylation reduction protocol

The TCO-Tz Click PEG_{OX} protocol was modified to selectively investigate S-glutathionylation by substituting TCEP with 8 U/ml recombinant human glutaredoxin 2 (GRX2) (#ab82665, Abcam, UK), 5 mM reduced L-glutathione (GSH) (#G4251, Sigma, UK), 4 U/ml Baker's yeast (*S. cerevisiae*) glutathione reductase (GR; #G3664, Sigma, UK) and 1 mM NADPH (#10107824001, Sigma, UK) for 30 min at room temperature with gentle agitation. Excess GSH and NADPH were removed by passing samples through a 6000 kDa spin column before the TCO-Tz Click reaction was performed as described above.

2.1.5. Redox mobility shift assay

Click reacted samples were resolved by molecular mass at 100 V for ~90–120 min on a pre-cast 4–15% gradient gel (BioRad, UK, #4561085) in running buffer (25 mM Tris, 190 mM glycine, 0.1% SDS, pH 8.3). Gels were transferred onto a low auto-fluorescence 0.45 μM PDVF (BioRad, UK, #1620261) membrane at 100 V for 60 min in transfer buffer (25 mM Tris, 190 mM glycine, 10% methanol, pH 8.3). Membranes were blocked with 5% non-fat dry milk (NFDM) in PBS for at least 60 min at room temperature. Membranes were incubated with an anti-ATP5A mouse monoclonal primary antibody (Abcam, UK, #ab14748) at a concentration of 1 μg/ml (in 3% NFDM TBST) overnight at 4 °C with gentle agitation [60,61]. A fluorescent pre-absorbed Alexa Flour$^{(R)}$ 750 mouse secondary antibody was used (dilution: 1:2000 in 3% NDFM TBST; Abcam, UK, #ab175741). Fluorescent signals were captured on an Analytik Jena scanner using the appropriate filters (excitation: 678–748 nm; emission: 767–807 nm). Bands were quantified on proprietary VisionWorks™ software. Consistent with previous research [27], the amount of Click PEGylated ATP-α-F_1 (i.e., mass shifted) was compared to the amount of reduced protein to derive percentage ATP-α-F_1 oxidation, which was calculated as: % oxidised protein = [oxidised protein (sum of mass shifted bands)/total protein] x 100. A substituted equation was used for the reduced protein: reduced protein = [sum of mass shifted bands/total signal] x 100. Internally normalising the analysis obviated the need for a loading control because it rendered the analysis *within* as opposed to between lanes. This was advantageous since many common loading controls (e.g., GAPDH [62]) possess solvent exposed thiols, which would confound parallel analysis.

2.1.6. Statistical analysis

Normal distribution was assessed using the D'Agostino-Pearson and Shapiro-Wilk normality tests. Both tests revealed that relevant data sets were normally distributed (i.e., alpha > 0.05). Parametric testing was, therefore, justified. Click PEG_{OX} and Click PEG_{RED} data were analysed by a one way ANOVA to test differences between independent means with alpha < 0.05. Selective S-glutathionylation experiments were analysed by an unpaired (i.e., independent means) Student's t-test with alpha < 0.05. Differences in the contribution of the 5 and 10 kDa bands to the total mass shifted signal within a time point (e.g., 15 min post fertilisation) were analysed by a paired Student's t-test with alpha < 0.05. Statistical analysis was performed on GraphPad Prism version 6 (https://www.graphpad.com/). Data are presented as Mean (M) and standard deviation (SD).

3. Results

3.1. Click PEG_{OX} reveals substantial reversible ATP-α-F_1 oxidation before and after fertilisation

We modified the Click PEGylation oxidation (Click PEG_{OX}) method developed by Van Leeuwen et al. [26] for TCO-Tz Click chemistry by: (1) using NEM to irreversibly alkylate reduced thiols by Michael addition; (2) TCEP to reduce reversibly oxidised thiols; (3) TCO-PEG3-NEM to label newly reduced thiols by Michael addition; and (4) Tz-PEG5 treatment to initiate the inverse electron demand Diels Alder reaction that selectively mass shifts reversibly oxidised protein thiols [31–33] (see Fig. 1). The 3 PEG spacer was selected to improve TCO group solubility, flexibility and accessibility. ATP-α-F_1 is an excellent TCO-Tz Click PEGylation candidate because it is abundant in unfertilised *X. laevis* eggs [63], both cysteine residues (i.e., C^{244} and C^{294}) are conserved and reversible oxidation is biologically meaningful—it implies low mitochondrial ATP F_1-F_o synthase activity [47]. C^{294} occurs earlier in the linear amino acid sequence in *X. laevis* due to a small deletion, but C^{294} is used throughout to allow phylogenetic comparisons (see Fig. 2). We used Click PEG_{OX} to interrogate reversible ATP-α-F_1 oxidation in the unfertilised egg and embryo at 15 and 90 min post fertilisation. The 15 and 90 min time-points were selected to capture redox changes as soon as practically possible after fertilisation and the first embryonic cell cycle, respectively [34]. Click PEG_{OX} revealed that: ATP-α-F_1 is substantially oxidised in the unfertilised egg (65.9 ± 8.4%), as well as, at 15 min (64 ± 5%) and 90 min (64.9 ± 11.3%) post fertilisation (see Fig. 3). A one way ANOVA revealed no significant differences between time-points ($P = 0.8306$). To put the result in perspective: the median reversible oxidation of cysteine residues in the mammalian proteome is in the order of 5–12% [64]. Diamide failed to increase the reversible oxidation observed. Instead, diamide decreased reversible oxidation, which could reflect irreversible oxidation to TCEP irreducible species (e.g., sulfinic acids). The doublet mass shift shows both C^{244} and C^{294} are reversibly oxidised. However, the percentage contribution of the 5 kDa band to the total mass shifted signal was significantly greater than the 10 kDa band within each time-point (see Table 1). Differential reversible oxidation shows that a single thiol is preferentially oxidised, making it the major contributor to the bulk signal. Contrary to our experimental hypothesis, ATP-α-F_1 is subject to substantial (~65%) reversible oxidation before and after fertilisation in *X. laevis*.

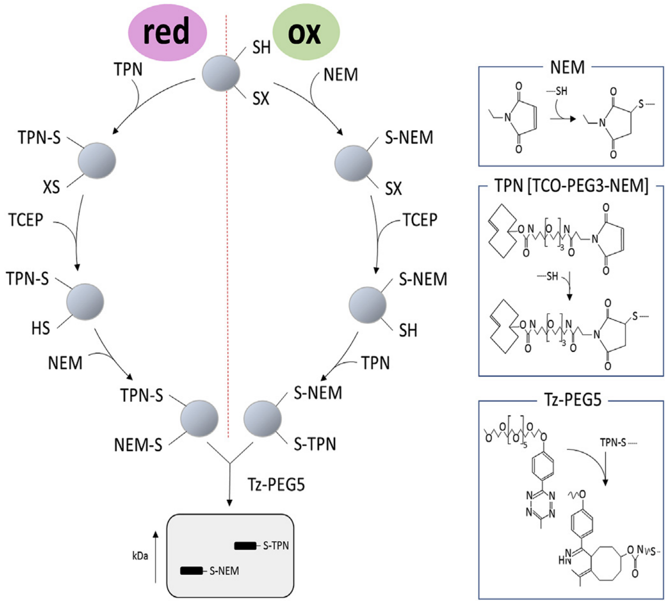

Fig. 1. Catalyst-free trans-cyclooctene-methyltetrazine (TCO-Tz) Click PEGylation schematic. The left side of the circle depicts the TCO-Tz Click PEGylation reduction (Click-PEG_{RED}) protocol wherein reduced thiols are labelled with TCO-3 polyethylene glycol (PEG)-maleimide (TCO-PEG3-NEM, TPN); (2) before 6-methyltetrazine PEG 5 kDa (Tz-PEG5) is added to initiate the inverse electron demand Diels alder reaction and thereby mass shift reduced thiols. An optional Tris (2-carboxyethyl)phosphine hydrochloride (TCEP) reduction step to reduce reversibly oxidised thiols before labelling them with N-ethylmaleimide (NEM) is depicted. The right side of the circle depicts the TCO-Tz Click PEGylation oxidation (Click-PEG_{OX}) protocol wherein (1) reduced thiols are labelled with NEM; (2) reversibly oxidised thiols are reduced with TCEP; (3) before being labelled with TCO-PEG3-NEM (TPN); and (4) 6 Tz-PEG5 is added to initiate the inverse electron demand Diels Alder reaction and thereby mass shift reversibly oxidised thiols. The insets on the far right depicts NEM mediated Michael addition (top), TPN mediated Michael addition to a reduced thiol (middle) and the inverse electron demand TCO-Tz Diels Alder reaction (bottom).

3.2. Click PEG_{RED} confirms substantial reversible ATP-α-F_1 oxidation before and after fertilisation

If ATP-α-F_1 is substantially oxidised before and after fertilisation, then mass shifting the reduced protein using a TCO-Tz Click PEG reduced (Click PEG_{RED}) protocol should yield the inverse result. Put differently, if ATP-α-F_1 is ~65% oxidised, then one would expect ~35% of the total protein to be mass shifted under Click PEG_{RED} conditions. To determine percentage ATP-α-F_1 reduction, we performed a Click PEG_{RED} redox mobility shift assay by using TCO-PEG3-NEM to irreversibly alkylate reduced thiols by Michael addition and Tz-PEG5 to selectively mass shift reduced protein thiols (see Fig. 1). Click PEG_{RED} showed that: ATP-α-F_1 is ~20–30% reduced before (29.1 ± 17.9%) and after fertilisation (15min: 23.6. ± 12.2%; 90 min: 31.1 ± 20.5%; see Fig. 4) in *X. laevis*. A one way ANOVA revealed no significant

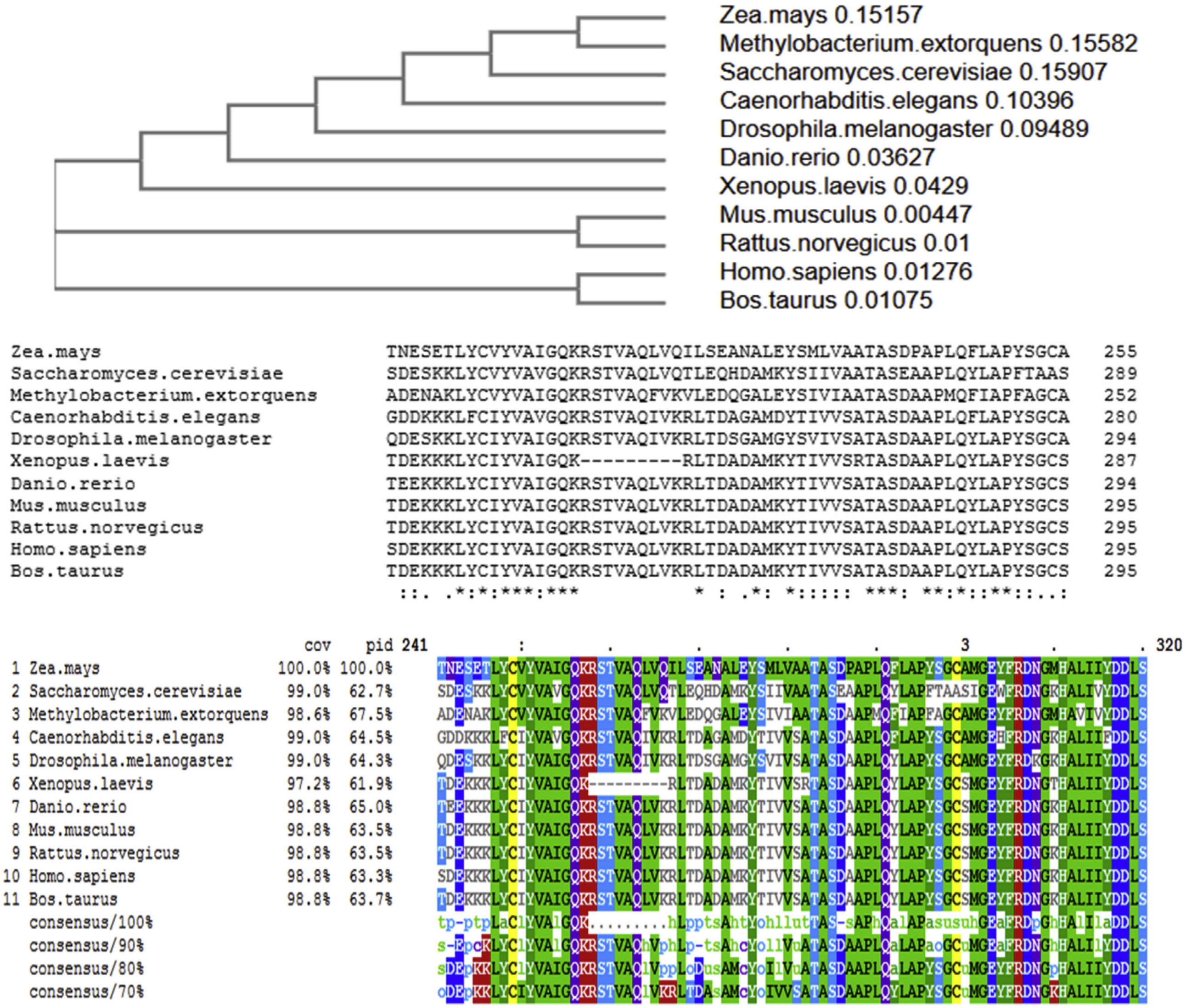

```
Zea.mays                        TNESETLYCVYVAIGQKRSTVAQLVQILSEANALEYSMLVAATASDPAPLQFLAPYSGCA   255
Saccharomyces.cerevisiae        SDESKKLYCVYVAVGQKRSTVAQLVQTLEQHDAMKYSIIVAATASEAAPLQYLAPFTAAS   289
Methylobacterium.extorquens     ADENAKLYCVYVAIGQKRSTVAQFVKVLEDQGALEYSIVIAATASDAAPMQFIAPFAGCA   252
Caenorhabditis.elegans          GDDKKKLFCIYVAVGQKRSTVAQIVKRLTDAGAMDYTIVVSATASDAAPLQFLAPYSGCA   280
Drosophila.melanogaster         QDESKKLYCIYVAIGQKRSTVAQIVKRLTDSGAMGYSVIVSATASDAAPLQYLAPYSGCA   294
Xenopus.laevis                  TDEKKKLYCIYVAIGQK---------RLTDADAMKYTIVVSRTASDAAPLQYLAPYSGCS   287
Danio.rerio                     TEEKKKLYCIYVAIGQKRSTVAQLVKRLTDADAMKYTIVVSATASDAAPLQYLAPYSGCS   294
Mus.musculus                    TDEKKKLYCIYVAIGQKRSTVAQLVKRLTDADAMKYTIVVSATASDAAPLQYLAPYSGCS   295
Rattus.norvegicus               TDEKKKLYCIYVAIGQKRSTVAQLVKRLTDADAMKYTIVVSATASDAAPLQYLAPYSGCS   295
Homo.sapiens                    SDEKKKLYCIYVAIGQKRSTVAQLVKRLTDADAMKYTIVVSATASDAAPLQYLAPYSGCS   295
Bos.taurus                      TDEKKKLYCIYVAIGQKRSTVAQLVKRLTDADAMKYTIVVSATASDAAPLQYLAPYSGCS   295
                                 ::. .*:*:***:***          * : .*: *::::: ***: **:*::**::..:
```

```
                                cov    pid 241          :         .         .         .         .         3         .         . 320
 1 Zea.mays                   100.0% 100.0%    TNESETLYCVYVAIGQKRSTVAQLVQILSEANALEYSMLVAATASDPAPLQFLAPYSGCAMGEYFRDNGMHALIIYDDLS
 2 Saccharomyces.cerevisiae    99.0%  62.7%    SDESKKLYCVYVAVGQKRSTVAQLVQTLEQHDAMKYSIIVAATASEAAPLQYLAPFTAASIGEWFRDNGKHALIVYDDLS
 3 Methylobacterium.extorquens 98.6%  67.5%    ADENAKLYCVYVAIGQKRSTVAQFVKVLEDQGALEYSIVIAATASDAAPMQFIAPFAGCAMGEYFRDNGMHAVIVYDDLS
 4 Caenorhabditis.elegans      99.0%  64.5%    GDDKKKLFCIYVAVGQKRSTVAQIVKRLTDAGAMDYTIVVSATASDAAPLQFLAPYSGCAMGEHFRDNGKHALIIFDDLS
 5 Drosophila.melanogaster     99.0%  64.3%    QDESKKLYCIYVAIGQKRSTVAQIVKRLTDSGAMGYSVIVSATASDAAPLQYLAPYSGCAMGEYFRDKGKHALIIYDDLS
 6 Xenopus.laevis              97.2%  61.9%    TDEKKKLYCIYVAIGQK---------RLTDADAMKYTIVVSRTASDAAPLQYLAPYSGCSMGEYFRDNGTHALIIYDDLS
 7 Danio.rerio                 98.8%  65.0%    TEEKKKLYCIYVAIGQKRSTVAQLVKRLTDADAMKYTIVVSATASDAAPLQYLAPYSGCSMGEYFRDNGKHALIIYDDLS
 8 Mus.musculus                98.8%  63.5%    TDEKKKLYCIYVAIGQKRSTVAQLVKRLTDADAMKYTIVVSATASDAAPLQYLAPYSGCSMGEYFRDNGKHALIIYDDLS
 9 Rattus.norvegicus           98.8%  63.5%    TDEKKKLYCIYVAIGQKRSTVAQLVKRLTDADAMKYTIVVSATASDAAPLQYLAPYSGCSMGEYFRDNGKHALIIYDDLS
10 Homo.sapiens                98.8%  63.3%    SDEKKKLYCIYVAIGQKRSTVAQLVKRLTDADAMKYTIVVSATASDAAPLQYLAPYSGCSMGEYFRDNGKHALIIYDDLS
11 Bos.taurus                  98.8%  63.7%    TDEKKKLYCIYVAIGQKRSTVAQLVKRLTDADAMKYTIVVSATASDAAPLQYLAPYSGCSMGEYFRDNGKHALIIYDDLS
   consensus/100%                              tp-ptpLaClYVAlGQK.........hLpptsAhtYohllutTAS-sAPhQalAPasusuhGEaFRDpGhHAlIlaDDLS
   consensus/90%                               s-EpcKLYClYVAlGQKRSTVAQhVphLp-tsAhcYollVuATASDAAPLQaLAPaoGCuMGEaFRDNGhHALIlYDDLS
   consensus/80%                               sDEpKKLYClYVAIGQKRSTVAQlVppLoDusAMcYoIlVuATASDAAPLQaLAPYSGCuMGEYFRDNGpHALIIYDDLS
   consensus/70%                               oDEpKKLYCIYVAIGQKRSTVAQlVKRLTDAsAMcYoIVVSATASDAAPLQYLAPYSGCuMGEYFRDNGKHALIIYDDLS
```

Fig. 2. Cysteine residues in *X. laevis* ATP-α-F_1 are evolutionary conserved. Top. Phylogenetic tree of the common model organisms selected. Middle. Multiple sequence alignments of ATP-α-F_1 derived from Clustal Omega (an open access online tool: https://www.ebi.ac.uk/Tools/msa/clustalo/). Bottom. Amino acid markup showing conserved cysteine residues in yellow. C^{294} occurs earlier in *X. laevis* due to a small deletion (see main text). Neighbouring amino acids surrounding C^{244} and C^{294} are highly conserved across phyla. (For interpretation of the references to colour in this figure legend, the reader is referred to the Web version of this article.)

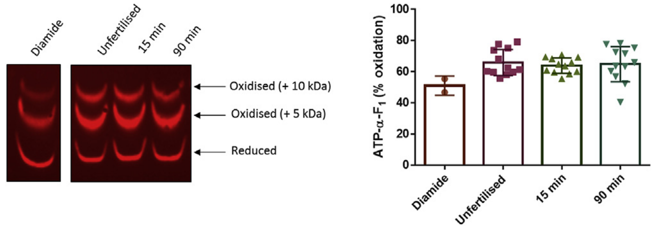

Fig. 3. ATP-α-F_1 is subject to substantial reversible oxidation before and after fertilisation in *X. laevis*. Left. Western blot image showing reversibly oxidised (i.e., mass shifted 5 and 10 kDa bands) relative to reduced ATP-α-F_1 (bottom band) before and after (15 and 90 min) fertilisation in *X. laevis*. Right. Percent reversible ATP-α-F_1 oxidation before ($n = 12$) and after fertilisation ($n = 12$) quantified. Each n = a pool of 5 eggs/embryos. The positive control refers to a diamide (50 mM for 30 min) treated sample. A one way ANOVA revealed no significant differences between time-points ($P = 0.8306$).

differences between time-points ($P = 0.6366$). Analogous to the reversible oxidation results, band analysis confirms that one thiol was preferentially reduced as evidenced by the differential contribution of the 5 kDa and 10 kDa signals (see Table 1). The reduced signal, therefore, primarily reflects the redox state of a single thiol. Click PEG_{RED} confirms substantial reversible ATP-α-F_1 oxidation before and after fertilisation.

3.3. ATP-α-F_1 is reversibly S-glutathionylated before and after fertilisation

To investigate reversible modification type, we substituted TCEP with recombinant glutaredoxin 2 (GRX2) to selectively reduce S-glutathionylated ATP-α-F_1 (see Fig. 5). Given the lack of difference between the two post-fertilisation time-points, only the 90 min time-point was selected. Selective reduction experiments reveal that: ~30–40% of the *total* ATP-α-F_1 protein is S-glutathionylated before (42.2 ± 12.6%) and after (36 ± 12%) fertilisation. The bottom band includes: reduced, reversibly oxidised (e.g., S-nitrosated) and irreversibly oxidised ATP-α-F_1. The small (~6%) decrease in S-glutationylated ATP-α-F_1 after fertilisation was statistically insignificant ($P = 0.8901$). Given ATP-α-F_1 is ~65% reversibly oxidised before and after fertilisation, we estimate S-glutathionylation accounts for 50–60% of the total reversible oxidation observed, making it the dominant oxidative modification type. The

Table 1
Percentage contribution of the 5 and 10 kDa band signal to the total mass shift observed by experiment. Data are M and SD (±). Significance is derived from a paired within time-point Student's t-test. *Denotes a statistically significant difference between the 5 and 10 kDa band within sample time-point. A one way ANOVA was used to assess statistical significance between time-points based on the 5 kDa signal in experiment 1 and 2. In experiment 3, an unpaired Student's t-test was used. No statistically significant differences were observed between time-points.

Time-point	5 kDa (%)	10 kDa (%)	Significance (P value)
Experiment 1: Oxidation			
Unfertilised eggs	64.4 ± 16.3	35.6 ± 16.3	0.0180*
Fertilised (15 min)	60.4 ± 13.0	39.6 ± 12.3	0.0135*
Fertilised (90 min)	64.3 ± 16.3	35.7 ± 19.4	0.0268*
Difference between time-points	n/a	n/a	0.7921
Experiment 2: Reduction			
Unfertilised eggs	74.7 ± 24.9	25.3 ± 24.9	0.0180*
Fertilised (15 min)	80.9 ± 23.3	19.1 ± 23.2	0.0040*
Fertilised (90 min)	71.2 ± 30.7	28.9 ± 30.7	0.0720
Difference between time-points	n/a	n/a	0.7362
Experiment 3: S-glutathionylation			
Unfertilised eggs	68.5 ± 7.3	31.5 ± 7.3	0.0001*
Fertilised (90 min)	74.0 ± 12.9	26.0 ± 12.9	0.0002*
Difference between time-points	n/a	n/a	0.2509

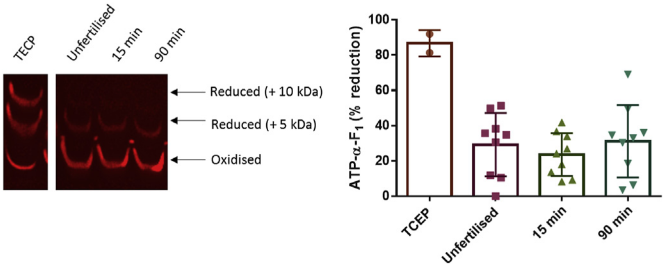

Fig. 4. Trans-cyclooctene-methyltetrazine (TCO-Tz) Click PEGylation reduction (Click-PEG$_{\text{RED}}$) confirms substantial reversible ATP-α-F$_1$ before and after fertilisation in *X. laevis*. Left. Western blot image showing reduced (i.e., mass shifted 5 and 10 kDa bands) relative to reversibly oxidised ATP-α-F$_1$ (bottom band) before and after (15 and 90 min) fertilisation in *X. laevis*. Right. Percent ATP-α-F$_1$ reduction before (n = 9) and after fertilisation (n = 9) in *X. laevis* quantified. Each n = a pool of 5 eggs/embryos. The positive control refers to a TCEP (50 mM for 30 min) treated sample. A one way ANOVA revealed no significant differences between time-points (P = 0.6366).

mass shifted doublet shows both C^{244} and C^{294} are S-glutathionylated. Analogous to the reversible oxidation result, the percentage contribution of the 5 kDa band to the total mass shifted signal was significantly greater than the 10 kDa band within each time-point (see Table 1). A single thiol (potentially C^{244}) is, therefore, preferentially S-glutathionylated likely due to greater solvent exposure during the catalytic cycle [65] (see Fig. 6). A selective chemical reduction strategy identifies S-gluthathionylation as the dominant reversible oxidation type before and after fertilisation in *X. laevis*.

4. Discussion

Unravelling how fundamental biological phenomena impact redox homeostasis by Western blotting requires new techniques to monitor protein thiol redox state [26,27]. To do so, one must overcome a perennial technical difficulty: the reduced and oxidised forms of most protein thiols possess similar electrophoretic mobility [27]. Building on a recent Cu$^+$ catalysed Click PEGylation method [26], we describe a novel catalyst-free TCO-Tz Click PEGylation approach to assess protein thiol redox state using Western blotting. Our approach enables one to estimate total reversible oxidation occupancy, differential occupancy between solvent exposed thiols, and establish reversible modification identity with selective reduction strategies (Table 2 lists key advantages and disadvantages of TCO-Tz Click PEGylation). TCO-Tz Click PEGylation may be a useful complementary technique for confirming redox proteomic findings [25]. For example, TCO-Tz Click PEGylation could be used to assess generator specific targets of mitochondrial $O_2^{\cdot-}/H_2O_2$ (i.e., cytochrome c-1 for complex I derived $O_2^{\cdot-}/H_2O_2$ produced by reverse electron transfer), which may enable investigators to infer the activity of a particular generator using an endogenous sentinel [2,66]. Click PEGylation relies on the primary antibody recognising the modified protein [26], but the bulky polymer itself and/or PEG-SDS micelles may obscure epitope recognition [27,58]. Potential solutions include using a polyclonal antibody and/or a smaller PEG polymer [26]. The latter strategy may be effective for small proteins (< 30 kDa) with one or two solvent exposed thiols. TCO-Tz Click PEGylation creates new opportunities to interrogate protein thiol redox state in health and disease, which is significant since evolutionary conserved cysteine residues tend to be functionally important [64,67,68].

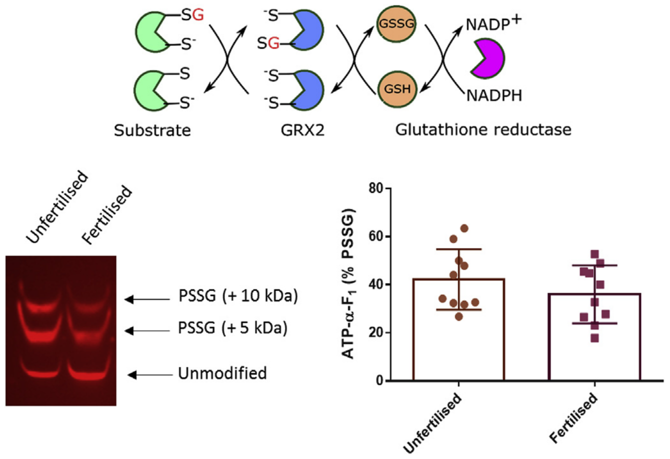

Fig. 5. ATP-α-F$_1$ is reversibly S-glutathionylated before and after fertilisation in *X. laevis*. Top. A reaction scheme depicting the selected chemical reduction strategy for S-glutathionylated proteins. In this scheme, GRX2 reduces S-glutathionylated proteins using glutathione (GSH) derived electrons. Glutathione reductase (GR) is used to reduce oxidised glutathione (GSSG) using NADPH. Left. Western blot image showing the S-glutathionylated (i.e., mass shifted 5 and 10 kDa bands) relative to total ATP-α-F$_1$ (bottom band) before and after (90 min) fertilisation in *X. laevis*. Right. Percent reversible ATP-α-F$_1$ S-glutathionylation (i.e., PSSG) before (n = 10) and after fertilisation (n = 10) in *X. laevis* quantified. Each n = a pool of 5 eggs/embryos. An independent unpaired Student's t-test revealed no statistically significant difference in reversible S-glutathionylation between time-points (P = 0.8901).

Underpinned by the pioneering work of Charles Manning Child [69] and reinvigorated by recent reports of fertilisation induced redox changes [34–37], the redox regulation of fertility is re-emerging as a key area of interest (reviewed in Refs. [70–72]). Petrova and colleagues [36] show that fertilisation alters the reduced thiol proteome, but whether fertilisation impacts reversible protein thiol oxidation is unknown. Our TCO-Tz Click PEGylation studies advance current understanding by revealing substantial reversible ATP-α-F$_1$ oxidation at C$^{244/294}$ before and after fertilisation. This novel result rationalises further work to understand how fertilisation impacts reversible thiol oxidation across the mitochondrial proteome. Substantial reversible ATP-α-F$_1$ oxidation implies low mitochondrial F$_1$-F$_o$ ATP synthase activity (i.e., low oligomycin sensitive respiration), consistent with suggestions that mitochondria in the unfertilised egg are functionally immature [73]. How reversible C$^{244/294}$ oxidation impairs catalysis is unresolved, but may involve intermolecular disulphide bond formation between C^{294}

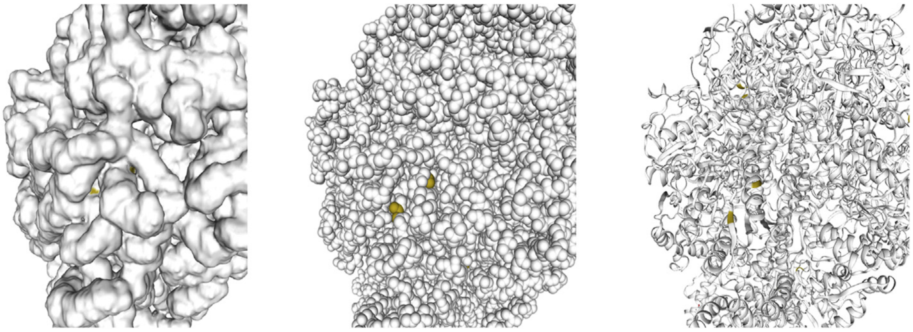

Fig. 6. Three dimensional molecular model of mitochondrial F_1-F_o ATP synthase in state 3a derived from Ref. [65] in *Bos taurus*. State 3a corresponds to a catalytic rotary state of the F_1 domain. Cysteine residues are highlighted in yellow, with C^{244} on the left and C^{294} on the right in each model display (left: surface; centre: space fill; right: ribbon). (For interpretation of the references to colour in this figure legend, the reader is referred to the Web version of this article.)

Table 2

Key advantages and disadvantages of TCO-Tz Click PEGylation.

Advantage	Disadvantage
● Hypothesis-driven. ● Can identify reversible oxidation occupancy and type. ● Catalyst-free. ● Selective and bio-orthogonal. ● Internally normalised. ● Flexible—method can be readily adapted. ● Democratic—makes use of readily available equipment and techniques. ● Cost and time efficient. ● Suitable as an orthogonal workflow to redox proteomics. ● Could be useful for studying the redox state of hydrophobic and/or difficult to digest proteins.	● Investigator bias given hypothesis driven nature. ● Relies on the antibody recognising the PEGylated protein. ● Biophysical interaction between SDS and PEG. ● Careful PEG, antibody and gel size selection is required. ● May be difficult to study proteins with many solvent exposed thiols. ● Inability to use technique in certain species when available epitopes are not conserved. ● Multiple bands preclude multiplexing.

and C^{103} of a proximal gamma F_1 sub-unit (ATP-γ-F_1) that impairs conformational flexibility [39,41]. Interestingly, intramolecular ATP-γ-F_1 disulphide crosslinks hold chloroplast ATP synthase inactive in darkness to prevent ATP hydrolysis until daylight restores catalysis by triggering thioredoxin mediated reduction [44,74]. Perhaps, *X. laevis* exploit a similar strategy to prevent wasteful F_1 mediated ATP hydrolysis. Recalcitrance of early *X. laevis* blastula to oligomycin [75], a canonical mitochondrial F_1-F_o ATP synthase inhibitor, could reflect preexisting inhibition by reversible oxidation. Persistent reversible ATP-α-F_1 oxidation after fertilisation implies low matrix reductase activity and/or equilibrium between the rate of reduction and oxidation. Reductive systems (e.g., GRX2) may only be partially operative, consistent with relatively weak embryonic antioxidant defence [76–78]. We propose that: $O_2^{\cdot-}/H_2O_2$ produced during oogenesis underlies the reversible oxidation observed as part of an ATP synthesis sensitive mitochondrial selection process [79]. Inhibitory ATP-α-F_1 oxidation may constrain mitochondrial F_o-F_1 ATP synthase activity until it is reversed to support metabolic differentiation later in development when the relevant reductive systems become operative [80].

Exploiting a GRX2 based selective reduction strategy, we show that: $C^{244/294}$ are S-glutathionylated before and after fertilisation in *X. laevis*. Successful deglutathionylation suggests ATP-α-F_1 may be a GRX2 substrate. ATP-α-F_1 S-glutathionylation is consistent with redox proteomic studies demonstrating $C^{244/294}$ S-glutathionylation *in vitro* in isolated mitochondrial and *in vivo* in canine hearts [46–48]. S-glutathionylation is the dominant oxidative modification type, accounting for ~50–60% of the reversible oxidation observed. The remaining 40–50% may comprise intermolecular disulphide bond formation since SOH and SNO species are relatively unstable [64,81]. Plausible chemical S-glutathionylation routes include: (1) un-catalysed addition of GSSG to a thiolate; (2) un-catalysed addition of GS^- to a thiyl radical, SOH or SNO species; (3) GRX2 and/or glutathione S-transferase catalysed conjugation of PSSG to a substrate thiol (reviewed in Refs. [40,82,83]). S-glutathionylation may block intermolecular disulphide crosslinks with ATP-γ-F_1 C^{103}. S-glutathionylation still correlates with impaired enzyme activity [40], but may make it easier to reactivate the enzyme if disulphide crosslinks pose steric challenges and/or aggregate. S-glutathionylation may also protect $C^{244/294}$ from irreversible oxidation to sulfinic and sulfonic acids [13]. Intriguingly, deglutathionylation of ATP-α-F_1 and other proteins may contribute to the increase in the reduced glutathione pool that occurs after fertilisation [84,85]. Further studies are, however, required to investigate the scale of the embryonic S-glutathionylated proteome and whether deglutathionylation contributes to developmental fluxes in reduced glutathione availability. TCO-Tz Click PEGylation protocols can be readily adapted by substituting generic for selective reductants to unveil the dominant oxidative modification type.

5. Conclusion

We describe a novel catalyst-free TCO-Tz Click PEGylation approach to assess protein thiol redox state by mass shifting the reduced or oxidised form as desired. Knowledge of how fertilisation—a key biological phenomenon—impacts matrix protein thiol redox state is fragmentary. To advance current understanding, we used TCO-Tz Click PEGylation to study the mitochondrial F_1-F_o ATP synthase by assessing the redox state of the essential cognate sub-unit ATP-α-F_1 in *X. laevis*. Three key novel findings are that: (1) ATP-α-F_1 is substantially reversibly oxidised at evolutionary conserved cysteine residues (i.e., $C^{244/C294}$) before and after fertilisation; and (2) S-glutathionylation is the dominant oxidative modification type; (3) a single thiol is preferentially oxidised likely due to greater solvent exposure during the catalytic cycle. Substantial reversible ATP-α-F_1 oxidation before and after fertilisation is biologically meaningful because it implies low mitochondrial F_1-F_o ATP synthase activity. Catalyst-free TCO-Tz Click PEGylation is a valuable new tool to interrogate protein thiol redox state in health and disease.

Acknowledgements

J.N.C., E.J.F., and H.H. gratefully acknowledge Highlands and Islands Enterprise (HMS 9353763) funding. The EXRC is funded by the Wellcome Trust (212942/Z/18/Z) and BBSRC (BB/R014841/1).

Appendix A. Supplementary data

Supplementary data to this article can be found online at https://doi.org/10.1016/j.redox.2019.101258.

Author contributions

Conceptualization, J.N.C. & H·H.; Methodology, J.N·C.; Investigation, J.N·C., E.J.F., M.T.V.M., & A.N.; Writing – Original Draft, J.N·C; Writing – Review & Editing, ALL; Funding Acquisition, J.N·C., H·H., and M.G.

References

[1] M.P. Murphy, How mitochondria produce reactive oxygen species, Biochem. J. 417 (2009) 1–13, https://doi.org/10.1042/BJ20081386.

[2] M.D. Brand, Mitochondrial generation of superoxide and hydrogen peroxide as the source of mitochondrial redox signaling, Free Radic. Biol. Med. 100 (2016) 14–31, https://doi.org/10.1016/j.freeradbiomed.2016.04.001.

[3] Y. Collins, E.T. Chouchani, A.M. James, K.E. Menger, H.M. Cocheme, M.P. Murphy, Mitochondrial redox signalling at a glance, J. Cell Sci. 125 (2012) 1837, https://doi.org/10.1242/jcs.110486.

[4] K.S. Echtay, D. Roussel, J. St-Pierre, M.B. Jekabsons, S. Cadenas, J.A. Stuart, J.A. Harper, S.J. Roebuck, A. Morrison, S. Pickering, J.C. Clapham, M.D. Brand, Superoxide activates mitochondrial uncoupling proteins, Nature 415 (2002) 96–99, https://doi.org/10.1038/415096a.

[5] M. Giorgio, M. Trinei, E. Migliaccio, P. Pelicci, Hydrogen peroxide: a metabolic by-product or a common mediator of ageing signals? Nat. Rev. Mol. Cell Biol. 8 (2007) 722–728, https://doi.org/10.1016/j.redox.2014.07.003.

[6] J.N. Cobley, M.-L. Fiorello, D.M. Bailey, 13 reasons why the brain is susceptible to oxidative stress, Redox Biol 15 (2018) 490–503.

[7] R.J. Mailloux, Teaching the fundamentals of electron transfer reactions in mitochondria and the production and detection of reactive oxygen species, Redox Biol 4 (2015) 381–398, https://doi.org/10.1016/j.redox.2015.02.001.

[8] L.A. Sena, N.S. Chandel, Physiological roles of mitochondrial reactive oxygen species, Mol. Cell 48 (2012) 158–166, https://doi.org/10.1016/j.molcel.2012.09.025.

[9] C.C. Winterbourn, D. Metodiewa, Reactivity of biologically important thiol compounds with superoxide and hydrogen peroxide, Free Radic. Biol. Med. 27 (1999) 322–328, https://doi.org/10.1016/S0891-5849(99)00051-9.

[10] C.C. Winterbourn, M.B. Hampton, Thiol chemistry and specificity in redox signaling, Free Radic. Biol. Med. 45 (2008) 549–561, https://doi.org/10.1016/j.freeradbiomed.2008.05.004.

[11] S. Stöcker, K. Van Laer, A. Mijuskovic, T.P. Dick, The conundrum of hydrogen peroxide signaling and the emerging role of peroxiredoxins as redox relay hubs, Antioxidants Redox Signal. 28 (2018) 558–573, https://doi.org/10.1089/ars.2017.7162.

[12] M. Lo Conte, K.S. Carroll, The redox biochemistry of protein sulfenylation and, J. Biol. Chem. 288 (2013) 26480–26488, https://doi.org/10.1074/jbc.R113.467738.

[13] M.P. Murphy, Mitochondrial thiols in antioxidant protection and redox signaling: distinct roles for glutathionylation and other thiol modifications, Antioxidants Redox Signal. 16 (2012) 476–495, https://doi.org/10.1089/ars.2011.4289.

[14] K.M. Holmström, T. Finkel, Cellular mechanisms and physiological consequences of redox-dependent signalling, Nat. Rev. Mol. Cell Biol. 15 (2014) 411–421, https://doi.org/10.1038/nrm3801.

[15] J. Yang, K.S. Carroll, D.C. Liebler, The expanding landscape of the thiol redox proteome, Mol. Cell. Proteom. 15 (2016) 1–11, https://doi.org/10.1074/mcp.O115.056051.

[16] D.T. Hess, A. Matsumoto, S.-O.O. Kim, H.E. Marshall, J.S. Stamler, Protein S-nitrosylation: purview and parameters, Nat. Rev. Mol. Cell Biol. 6 (2005) 150–166, https://doi.org/10.1038/nrm1569.

[17] R.J. Mailloux, J.R. Treberg, Protein S-glutathionlyation links energy metabolism to redox signaling in mitochondria, Redox Biol 8 (2016) 110–118, https://doi.org/10.1016/j.redox.2015.12.010.

[18] H.J. Forman, M. Maiorino, F. Ursini, Signaling functions of reactive oxygen species, Biochemistry 49 (2010) 835–842, https://doi.org/10.1021/bi9020378.

[19] S. Parvez, M.J.C. Long, J.R. Poganik, Y. Aye, Redox signaling by reactive electrophiles and oxidants, Chem. Rev. 118 (2018) 8798–8888, https://doi.org/10.1021/acs.chemrev.7b00698.

[20] C.E. Paulsen, K.S. Carroll, Cysteine-mediated redox Signaling : chemistry , biology , and tools for discovery, Chem. Rev. 133 (2013) 4633–4679, https://doi.org/10.1021/cr300163e.

[21] S. Dröse, U. Brandt, I. Wittig, Mitochondrial respiratory chain complexes as sources and targets of thiol-based redox-regulation, Biochim. Biophys. Acta Protein Proteonomics 1844 (2014) 1344–1354, https://doi.org/10.1016/j.bbapap.2014.02.006.

[22] A. Galkin, B. Meyer, I. Wittig, M. Karas, H. Schägger, A. Vinogradov, U. Brandt, Identification of the mitochondrial ND3 subunit as a structural component involved in the active/deactive enzyme transition of respiratory complex I, J. Biol. Chem. 283 (2008) 20907–20913, https://doi.org/10.1074/jbc.M803190200.

[23] E.T. Chouchani, V.R. Pell, E. Gaude, D. Aksentijević, S.Y. Sundier, E.L. Robb, A. Logan, S.M. Nadtochiy, N.J. Emily, A.C. Smith, F. Eyassu, R. Shirley, C. Hu, A.J. Dare, A.M. James, S. Rogatti, R.C. Hartley, S. Eaton, S.H. Ana, P.S. Brookes, S.M. Davidson, M.R. Duchen, K. Saeb-parsy, Ischaemic accumulation of succinate controls reperfusion injury through mitochondrial ROS, Nature 515 (2014) 431–435, https://doi.org/10.1038/nature13909.Ischaemic.

[24] E.T. Chouchani, C. Methner, S.M. Nadtochiy, A. Logan, R. Victoria, S. Ding, A.M. James, H.M. Cochemé, J. Reinhold, K.S. Lilley, L. Partridge, I.M. Fearnley, A.J. Robinson, R.C. Hartley, R.A.J. Smith, T. Krieg, P.S. Brookes, M.P. Murphy, Cardioprotection by S-nitrosation of a cysteine switch on mitochondrial complex I, Nat. Med. 19 (2013) 753–759, https://doi.org/10.1038/nm.3212.Cardioprotection.

[25] J.N. Cobley, G.K. Sakellariou, H. Husi, B. Mcdonagh, Proteomic strategies to unravel age-related redox signalling defects in skeletal muscle, Free Radic. Biol. Med. 132 (2019) 24–32, https://doi.org/10.1016/j.freeradbiomed.2018.09.012.

[26] L.A.G. van Leeuwen, E.C. Hinchy, M.P. Murphy, E.L. Robb, H.M. Cochemé, Click-PEGylation – a mobility shift approach to assess the redox state of cysteines in candidate proteins, Free Radic. Biol. Med. 108 (2017) 374–382, https://doi.org/10.1016/j.freeradbiomed.2017.03.037.

[27] J.R. Burgoyne, O. Oviosu, P. Eaton, The PEG-switch assay: a fast semi-quantitative method to determine protein reversible cysteine oxidation, J. Pharmacol. Toxicol. Methods 68 (2013) 297–301, https://doi.org/10.1016/j.vascn.2013.07.001.

[28] V. Rostovtsev, L. Green, V. Fokin, K. Sharpless, A stepwise huisgen cycloaddition process catalyzed by copper (I): regioselective ligation of azides and terminal alkynes, Angew. Chem. Int. Ed. 41 (2002) 2596–2599, https://doi.org/10.1021/jo011148j.

[29] B. Halliwell, J.M.C. Gutteridge, Free Radicals in Biology & Medicine, fifth ed., Oxford University Press, 2015.

[30] J. Jewett, C. Bertozzi, Cu-free click cycloaddition reactions in chemical biology, Chem. Soc. Rev. 39 (2010) 1272–1279, https://doi.org/10.1016/j.dci.2009.07.003.Characterization.

[31] O. Diels, K. Alder, Synthesen in der hydroaromatischen Reihe, Justus Liebigs Ann. Chem. 460 (1928) 98–122.

[32] B.L. Oliveira, Z. Guo, G.J.L. Bernardes, Inverse electron demand Diels-Alder reactions in chemical biology, Chem. Soc. Rev. 46 (2017) 4895–4950, https://doi.org/10.1039/c7cs00184c.

[33] M.L. Blackman, M. Royzen, J.M. Fox, Tetrazine Ligation : fast bioconjugation based on inverse-electron-demand Diels - alder reactivity, J. Am. Chem. Soc. 130 (2008) 13518–13519.

[34] Y. Han, S. Ishibashi, J. Iglesias-Gonzalez, Y. Chen, N.R. Love, E. Amaya, Ca2+-Induced mitochondrial ROS regulate the early embryonic cell cycle, Cell Rep. 22 (2018) 218–231, https://doi.org/10.1016/j.celrep.2017.12.042.

[35] R. Dumollard, J. Carroll, M.R. Duchen, K. Campbell, K. Swann, Mitochondrial function and redox state in mammalian embryos, Semin. Cell Dev. Biol. 20 (2009) 346–353, https://doi.org/10.1016/j.semcdb.2008.12.013.

[36] B. Petrova, K. Liu, C. Tian, M. Kitaoka, E. Freinkman, J. Yang, T.L. Orr-Weaver, Dynamic redox balance directs the oocyte-to-embryo transition via developmentally controlled reactive cysteine changes, Proc. Natl. Acad. Sci. Unit. States Am. 115 (2018) 201807918, https://doi.org/10.1073/pnas.1807918115.

[37] R. Dumollard, Sperm-triggered [Ca2+] oscillations and Ca2+ homeostasis in the mouse egg have an absolute requirement for mitochondrial ATP production, Development 131 (2004) 3057–3067, https://doi.org/10.1242/dev.01181.

[38] L. Vastag, P. Jorgensen, L. Peshkin, R. Wei, J.D. Rabinowitz, M.W. Kirschner, Remodeling of the metabolome during early frog development, PLoS One 6 (2011), https://doi.org/10.1371/journal.pone.0016881.

[39] N. Kaludercic, V. Giorgio, The dual function of reactive oxygen/nitrogen species in bioenergetics and cell death: the role of ATP synthase, Oxid. Med. Cell. Longev. (2016), https://doi.org/10.1155/2016/3869610 2016.

[40] R.J. Mailloux, W.G. Willmore, S-glutathionylation reactions in mitochondrial function and disease, Front. Cell Dev. Biol. 2 (2014) 1–17, https://doi.org/10.3389/fcell.2014.00068.

[41] S.B. Wang, C.I. Murray, H.S. Chung, J.E. Van Eyk, Redox regulation of mitochondrial ATP synthase, Trends Cardiovasc. Med. 23 (2013) 18, https://doi.org/10.1016/j.tcm.2012.08.005.

[42] J.P. Abrahams, A.G.W. Leslie, R. Lutter, J.E. Walker, Structure at 2 . 8 A resolution of F1 · ATPase from bovine heart mitochondria, Nature 370 (1994) 621–628.

[43] P. Mitchell, Coupling of phosphorylation to electron and hydrogen transfer by a chemi-osmotic type of mechanism, Nature 191 (1961) 144–148, https://doi.org/10.1038/192452a0.

[44] J.E. Walker, S.J. Walker, Keilin memorial lecture keilin memorial lecture the ATP synthase : the understood , the uncertain and the unknown, Biochem. Soc. Trans. 41 (2013) 1–16, https://doi.org/10.1042/BST20110773.

[45] R.I. Menz, J.E. Walker, A.G.W. Leslie, Structure of bovine mitochondrial F 1 -ATPase with nucleotide bound to all three catalytic Sites : implications for the mechanism of rotary catalysis, Cell 106 (2001) 331–341.

[46] M.B. West, B.G. Hill, Y.T. Xuan, A. Bhatnagar, Protein glutathiolation by nitric oxide: an intracellular mechanism regulating redox protein modification, FASEB J. 20 (2006) 1715–1717, https://doi.org/10.1096/fj.06-5843fje.

[47] S.B. Wang, D.B. Foster, J. Rucker, B. O'Rourke, D.A. Kass, J.E. Van Eyk, Redox regulation of mitochondrial ATP synthase: implications for cardiac resynchronization therapy, Circ. Res. 109 (2011) 750–757, https://doi.org/10.1161/CIRCRESAHA.111.246124.

[48] J. Garcia, D. Han, H. Sancheti, L.P. Yap, N. Kaplowitz, E. Cadenas, Regulation of mitochondrial glutathione redox status and protein glutathionylation by respiratory substrates, J. Biol. Chem. 285 (2010) 39646–39654, https://doi.org/10.1074/jbc.M110.164160.

[49] J. Sun, T. Nguyen, A.M. Aponte, S. Menazza, M.J. Kohr, D.M. Roth, H.H. Patel, E. Murphy, C. Steenbergen, Ischaemic preconditioning preferentially increases protein S-nitrosylation in subsarcolemmal mitochondria, Cardiovasc. Res. 106

(2015) 227–236, https://doi.org/10.1093/cvr/cvv044.

[50] A.M. Session, Y. Uno, T. Kwon, J. a Chapman, A. Toyoda, S. Takahashi, A. Fukui, A. Hikosaka, A. Suzuki, M. Kondo, S.J. Van Heeringen, I. Quigley, S. Heinz, H. Ogino, H. Ochi, U. Hellsten, J.B. Lyons, O. Simakov, N. Putnam, J. Stites, J.B. Wallingford, Y. Ito, M. Asashima, N. Ueno, Y. Matsuda, G.J.C. Veenstra, Genome evolution in the allotetraploid frog *Xenopus laevis*, Nature 538 (2016) 1–15, https://doi.org/10.1038/nature19840.

[51] R.M. Harland, R.M. Grainger, Xenopus research: metamorphosed by genetics and genomics, Trends Genet. 27 (2011) 507–515, https://doi.org/10.1016/j.tig.2011.08.003.

[52] E. Sidlauskaite, J.W. Gibson, I.L. Megson, P.D. Whitfield, A. Tovmasyan, I. Batinic-Haberle, M.P. Murphy, P.R. Moult, J.N. Cobley, Mitochondrial ROS cause motor deficits induced by synaptic inactivity: implications for synapse pruning, Redox Biol 16 (2018) 344–351, https://doi.org/10.1016/j.redox.2018.03.012.

[53] M. Guille, Microinjection into Xenopus oocytes and embryos, Mol. Methods Dev. Biol. 127 (1999) 111–123.

[54] H.L. Sive, R.M. Grainger, R.M. Harland, Early Development of *Xenopus laevis*: A Laboratory Manual, first ed., Cold Spring Harbor Laboratory Press, New York, 2000.

[55] C. Kilkenny, W.J. Browne, I.C. Cuthill, M. Emerson, D.G. Altman, Improving bioscience research Reporting : the ARRIVE guidelines for reporting animal research, PLoS Biol. 8 (2010) 6–10, https://doi.org/10.1371/journal.pbio.1000412.

[56] M.M. Bradford, A rapid and sensitive method for the quantitation of microgram quantities of protein utilizing the principle of protein-dye binding, Anal. Biochem. 72 (1976) 248–254, https://doi.org/10.1016/0003-2697(76)90527-3.

[57] K. Tyagarajan, E. Pretzer, J.E. Wiktorowicz, Thiol-reactive dyes for fluorescence labeling of proteomic samples, Electrophoresis 24 (2003) 2348–2358, https://doi.org/10.1002/elps.200305478.

[58] C.Y. Zheng, G. Ma, Z. Su, Native PAGE eliminates the problem of PEG-SDS interaction in SDS-PAGE and provides an alternative to HPLC in characterization of protein PEGylation, Electrophoresis 28 (2007) 2801–2807, https://doi.org/10.1002/elps.200600807.

[59] U. Laemmli, Cleavage of structural proteins during the assembly of the head of bacteriophage T4, Nature 277 (1970) 680–685.

[60] J.N. Cobley, J.D. Bartlett, A. Kayani, S.W. Murray, J. Louhelainen, T. Donovan, S. Waldron, W. Gregson, J.G. Burniston, J.P. Morton, G.L. Close, PGC-1a transcriptional response and mitochondrial adaptation to acute exercise is maintained in skeletal muscle of sedentary elderly males, Biogerontology 13 (2012) 621–631, https://doi.org/10.1007/s10522-012-9408-1.

[61] J.N. Cobley, G.K. Sakellariou, D.J. Owens, S. Murray, S. Waldron, W. Gregson, W.D. Fraser, J.G. Burniston, L.A. Iwanejko, A. McArdle, J.P. Morton, M.J. Jackson, G.L. Close, Lifelong training preserves some redox-regulated adaptive responses after an acute exercise stimulus in aged human skeletal muscle, Free Radic. Biol. Med. 70 (2014) 23–32, https://doi.org/10.1016/j.freeradbiomed.2014.02.004.

[62] D. Peralta, A.K. Bronowska, B. Morgan, É. Dóka, K. Van Laer, P. Nagy, F. Gräter, T.P. Dick, A proton relay enhances H2O2 sensitivity of GAPDH to facilitate metabolic adaptation, Nat. Chem. Biol. 11 (2015) 156–163, https://doi.org/10.1038/nchembio.1720.

[63] M. Wühr, R.M. Freeman, M. Presler, M.E. Horb, L. Peshkin, S.P. Gygi, M.W. Kirschner, Deep proteomics of the *Xenopus laevis* egg using an mRNA-derived reference database, Curr. Biol. 24 (2014) 1467–1475, https://doi.org/10.1016/j.cub.2014.05.044.

[64] Y.-M. Go, J.D. Chandler, D.P. Jones, The cysteine proteome, Free Radic. Biol. Med. 84 (2015) 227–245, https://doi.org/10.1016/j.freeradbiomed.2015.03.022.

[65] A. Zhou, A. Rohou, D.G. Schep, J. V Bason, M.G. Montgomery, J.E. Walker, N. Grigorieff, Structure and conformational states of the bovine mitochondrial ATP synthase by cryo-EM, Elife 4 (2015) e10180, , https://doi.org/10.7554/eLife.10180.

[66] L. Bleier, I. Wittig, H. Heide, M. Steger, U. Brandt, S. Drose, Generator-specific targets of mitochondrial reactive oxygen species, Free Radic. Biol. Med. 78 (2015) 1–10, https://doi.org/10.1016/j.freeradbiomed.2014.10.511.

[67] S.M. Marino, V.N. Gladyshev, Cysteine function governs its conservation and degeneration and restricts its utilization on protein surfaces, J. Mol. Biol. 404 (2010) 902–916, https://doi.org/10.1016/j.jmb.2010.09.027.

[68] E. Weerapana, C. Wang, G.M. Simon, F. Richter, S. Khare, M.B.D. Dillon, D.A. Bachovchin, K. Mowen, D. Baker, B.F. Cravatt, Quantitative reactivity profiling predicts functional cysteines in proteomes, Nature 468 (2010) 790–795, https://doi.org/10.1038/nature09472.

[69] C.M. Child, Patterns and Problems in Development, Chicago University Press, Chicago, 1947.

[70] C. Rampon, M. Volovitch, A. Joliot, S. Vriz, Hydrogen peroxide and redox regulation of developments, Antioxidants 7 (2018) 159, https://doi.org/10.3390/antiox7110159.

[71] N.W. Blackstone, Multicellular redox regulation: integrating organismal biology and redox chemistry, Bioessays 28 (2006) 72–77, https://doi.org/10.1002/bies.20337.

[72] N.W. Blackstone, Redox control and the evolution of multicellularity, Bioessays 22 (2000) 947–953, https://doi.org/10.1002/1521-1878(200010)22:10<947::AID-BIES10>3.0.CO;2-W.

[73] J.F. Allen, Separate sexes and the mitochondrial theory of ageing, J. Theor. Biol. 180 (1996) 135–140.

[74] C.M. Nalins, R.E. Mccarty, Role of a disulfide bond in the y subunit in activation of the ATPase of chloroplast coupling factor 1 ” P-, J. Biol. Chem. 259 (1984) 7275–7280.

[75] R. Gibeaux, R. Acker, M. Kitaoka, G. Georgiou, I. van Kruijsbergen, B. Ford, E.M. Marcotte, D.K. Nomura, T. Kwon, G.J.C. Veenstra, R. Heald, Paternal chromosome loss and metabolic crisis contribute to hybrid inviability in Xenopus, Nature 553 (2018) 337–341, https://doi.org/10.1038/nature25188.

[76] K.F.S. Bell, B. Al-Mubarak, M.-A. Martel, S. McKay, N. Wheelan, P. Hasel, N.M. Márkus, P. Baxter, R.F. Deighton, A. Serio, B. Bilican, S. Chowdhry, P.J. Meakin, M.L.J. Ashford, D.J.A. Wyllie, R.H. Scannevin, S. Chandran, J.D. Hayes, G.E. Hardingham, Neuronal development is promoted by weakened intrinsic antioxidant defences due to epigenetic repression of Nrf2, Nat. Commun. 6 (2015) 7066, https://doi.org/10.1038/ncomms8066.

[77] P.A. Dennery, Oxidative stress in development: nature or nurture? Free Radic. Biol. Med. 49 (2010) 1147–1151, https://doi.org/10.1016/j.freeradbiomed.2010.07.011.

[78] J.N. Cobley, Synapse pruning: mitochondrial ROS with their hands on shears, Bioessays 40 (2018) e1800031, , https://doi.org/10.1002/bies.201800031.

[79] T. Lieber, S. Jeedigunta, J. Palozzi, R. Lehmann, T. Hurd, Removal of deleterious mtDNA in the germline, Nature (2019), https://doi.org/10.1038/s41586-019-1213-4.

[80] M. Agathocleous, N.K. Love, O. Randlett, J.J. Harris, J. Liu, A.J. Murray, W.A. Harris, Metabolic differentiation in the embryonic retina, Nat. Cell Biol. 14 (2012) 859–864, https://doi.org/10.1038/ncb2531.

[81] K. Wolhuter, P. Eaton, How widespread is stable protein S-nitrosylation as an end-effector of protein regulation? Free Radic. Biol. Med. 109 (2017) 156–166, https://doi.org/10.1016/j.freeradbiomed.2017.02.013.

[82] T.R. Hurd, N.J. Costa, C.C. Dahm, S.M. Beer, S.E. Brown, A. Filipovska, M.P. Murphy, Glutathionylation of mitochondrial proteins, Antioxidants Redox Signal. 7 (2005) 999–1010, https://doi.org/10.1089/ars.2007.1811.

[83] J.J. Mieyal, M.M. Gallogly, S. Qanungo, E. Sabens, M. Shelton, Molecular mechanisms and clinical implications of reversible protein S-glutathionylation, Antioxidants Redox Signal. 10 (2008) 1943–1988, https://doi.org/10.1089/ars.2008.2089.

[84] J.M. Hansen, C. Harris, Glutathione during embryonic development, Biochim. Biophys. Acta Gen. Subj. 1850 (2015) 1527–1542, https://doi.org/10.1016/j.bbagen.2014.12.001.

[85] A.R. Timme-Laragy, J.V. Goldstone, B.R. Imhoff, J.J. Stegeman, M.E. Hahn, J.M. Hansen, Glutathione redox dynamics and expression of glutathione-related genes in the developing embryo, Free Radic. Biol. Med. 65 (2013) 89–101, https://doi.org/10.1016/j.freeradbiomed.2013.06.011.